Electric Power Systems Research 190 (2021) 106663

Contents lists available at ScienceDirect

Electric Power Systems Research

journal homepage: www.elsevier.com/locate/epsr

Control of distribution grids with storage using nested Benders' decomposition

Marco Giuntoli*, Milos Subasic, Susanne Schmitt

ABB Corporate Research Germany, Ladenburg, Germany

ARTICLE INFO

Keywords:
Optimal power flow
Distribution grid
Storage
Nested Benders' decomposition

ABSTRACT

The rapid spread of the renewable energy sources (RES) in conjunction with an increase of electric vehicles and prosumer technology in distribution systems pushes the distribution system operators to actively and economically manage and control the grid. In order to treat the unpredictable nature of RES, the operators increasingly resort to battery energy storage system (BESS). Coupled with the control functionalities such as optimal power flow (OPF), BESS can provide a leverage in grid management. The paper proposes an innovative approach to multi-period OPF based on Nested Benders' Decomposition to properly model the multi-period constraints of the energy level of BESS. In our approach we are assessing the convergence of the nonlinear and nonconvex AC power flow using NBD. Finally, the performance of the methodology in terms of objective function values and computational complexity is evaluated through the series of test cases based on various IEEE distribution testbeds.

1. Introduction

The rapid development of new energy technologies made possible that more and more renewable energy sources (RES) are being integrated into power distribution systems in the form of distributed generations (DG). On the other hand, poor range and limited attractiveness have long been the two biggest bottlenecks to electric vehicle (EV) uptake. This is changing due to fact that more than 300 new, feature-laden EV models will have their debut before 2025. On base of EV adoption study as reported in [1], there will be around 120 million of EVs on the road by 2030. To support such a large number of vehicles, appropriate charging infrastructure will be necessary. Finally, number of residential and commercial prosumers is rising, changing the energy picture of the distribution grid dramatically. It is no wonder that power converter interfaced DG systems, electric vehicle (EV) charging stations and prosumer technologies coupled with the state-of-the-art communication and control techniques have been recognized to play crucial roles in the development of future energy picture of the power grid, especially its distribution portion.

On the other hand, the increasing proportion of integration of these technologies is posing many challenges to the traditional distribution grid management. Due to high-permeability to dynamic loads and distributed PV, power distribution grids may be exposed to increased voltage levels, short circuit current increases, power supply reliability and power quality deterioration phenomena. In order to solve the above problems, the traditional distribution grid has gradually changed from passive mode to active control modes in an attempt to accommodate the trend from the "one-way" to "multi-direction" flows. One of the measures that engineers resort to counteract these problems is to limit RES penetration, which may result in significant energy curtailments. A means to assist the non-treatable nature of renewables is to implement battery energy storage system (BESS). Ideally BESS not only backs up and complements intermittent renewable sources; but along with an appropriate optimization model with forecasted scenarios, it can decrease uncertainty of renewable energy limited predictability. The BESS is a critical component of future distribution grids and is fundamental to the effective use of renewable resources [2]. BESS can increase the hosting capacity of distribution grids by providing required stabilization under high renewable penetration.

In transmission grids, planning and operational tools are well established. One of the fundamental and widely used types of algorithms utilized for control of the grids is the optimal power flow (OPF) algorithm. This algorithm uses the optimization methods to find the solution for power system variables [3]. Apart from operating in an economically optimal way, it is crucial for a power system to operate with respect to certain criteria that ensure security and reliability.

The optimal control of BESS cannot rely on a one snapshot optimization due to the multi-period constraints related to the energy level; therefore, sophisticated optimization techniques capable of handling multi-period problems should be applied. Nested Benders' decomposition

* Corresponding author.
E-mail addresses: marco.giuntoli@de.abb.com (M. Giuntoli), milos.subasic@de.abb.com (M. Subasic), susanne.schmitt@de.abb.com (S. Schmitt).

https://doi.org/10.1016/j.epsr.2020.106663
Received 30 September 2019; Received in revised form 8 April 2020; Accepted 1 August 2020
Available online 06 August 2020
0378-7796/

(NBD) is a well-known decomposition technique for large-scale optimization problems. One advantage of the algorithm is that convergence to the optimal solution can be achieved for linear problems as shown in [4]. More generally, convergence can be reached also for convex nonlinear problems. This was proven by author in [5] where nonlinear convex duality theory is employed to derive the natural families of cuts corresponding to those in Benders' case. In hydro-thermal scheduling, NBD has been used in order to decompose the multi-period problem along the time domain and enable parallel processing of the subproblems [6,7]. Moreover, NBD has already been proposed for solving power system expansion planning problems in [8,9]. Authors solved the problem at hand by using the approach characterized by linear disjunctive model to ensure the optimality of solution and by additional constraints and applying compromised approach of direct decomposition to sum of cuts and cuts themselves respectively. In [10] authors propose a solution to transmission-constrained unit commitment based on NBD by decomposing the problem at hand into a master problem and a subproblem. Master problem solves unit commitment without transmission constraints and the subproblem minimizes violations of transmission constraints. Finally, NBD is used to solve multiperiod transmission system OPF taking into consideration start-up and shut-down sequences of thermal plants in [11]. In [12] Benders' decomposition is applied to the security-constrained OPF problem, while the authors in [13] use NBD to solve a transmission planning problem as mixed-integer optimization problem.

To our best knowledge, NBD was never in past applied to solve AC-OPF in distribution systems in a multi-period manner to tackle the time linking of constraints phenomena due to BESS. This is the main contribution of our work. There are approaches for multi-period OPF in distribution grids with storage available, like e.g. [14]. However, the authors consider the holistic optimization problem without decomposition techniques.

2. Optimal power flow formulation

A nonlinear multi-period OPF problem for a time horizon T can in general be formulated as the task to minimize an objective function that consists of the sum of objective functions for the single time steps:

$$f(x) = \sum_{t=0}^{T} f_t(x_t) \tag{1}$$

One possible objective function is represented as the sum of generator dispatch costs in the system for a time horizon T:

$$\zeta = \sum_{t=0}^{T} \sum_{g=1}^{N_G} \beta_t^g P_t^g \tag{2}$$

Here N_G is the number of generators in the grid, P^g is the active power generated by the generator g, while β^g is the cost coefficient for the individual generators. Similarly, the objective function can be rewritten to correspond to grid losses by simply setting $\beta_t^g = 1$ for all generators and the entire time horizon. Alternative objective functions would be total voltage deviation or a combination of the ones listed.

Control variables are generation and storage setpoints, while state variables comprise voltage magnitudes and angles, active and reactive power flows over lines.

In this paper, for each point in time there is a set of inequality constraints modelling the physical limits of grid components such as the current limit of the line and the generator and storage variable bounds:

$$g_t(x_t) \leq 0, \quad \text{for } t = 0, \ \ldots, \ T \tag{3}$$

In addition, there is a set of equality constraints for each point in time. The following equation describes the active power balance for a node for all $t = 0, \ldots, T$:

$$-P_t(V_{n,t}, \theta_{n,t}) + P_{g,t} - P_{n,d,t} + P_{c,t}^s - P_{d,t}^s = 0 \tag{4}$$

Here, the subscripts n denotes the n-th node. The term $-P_t(V_{n,t}, \theta_{n,t})$ is the real power flow into the n-th node and v and θ are the voltage magnitude and phase, the term P_g is the power supplied by the g-th active source and the term P_d is the power demand. $P_{c,t}^s$ and $P_{d,t}^s$ are the power charged to/ discharged from the storage s at time t, respectively.

In the same way as for real, it is possible to describe the nodal reactive power balance:

$$-Q_t(V_{n,t}, \theta_{n,t}) + Q_{g,t} - Q_{n,d,t} = 0 \tag{5}$$

For a generic branch b and defining i as from-node and j as to-node, it is possible to describe the relationship between the current and voltage phasors as follows:

$$\begin{bmatrix} I_{i,t} \\ I_{j,t} \end{bmatrix} - \begin{bmatrix} \overline{y_{ii}}\delta_b^2 & \overline{y_{ij}}\delta_b e^{j\theta_{b,t}} \\ \overline{y_{ji}}\delta_b e^{-j\theta_{b,t}} & \overline{y_{ii}} \end{bmatrix} \begin{bmatrix} V_{i,t} \\ V_{j,t} \end{bmatrix} = 0 \tag{6}$$

Exploiting the symmetry of the model, the matrix component with subscript ii is equal to the component with jj and, in the same way, the component with ij is equal to the component with ji. Those values arise from the longitudinal and transversal susceptance and conductance parameters. The equations that describe a double bi-pole model are used to model the active and reactive power flow through the branches, and thus those flows are used inside the nodes power balance Eqs. (3) and (4).

In contrast to the grid related constraints described above, the presence of energy storage in the grid introduces time-coupling constraints. In particular, the energy storage state of charge depends linearly on the state of charge in the previous time step and the power charged/discharged from it:

$$E_t^s = E_{t-1}^s + e_c^s P_{c,t}^s - e_d^s P_{d,t}^s \quad t = 1, \ \ldots, T, \quad s = 1, \ \ldots, S \tag{7}$$

Here S is the total number of storages in the grid, E_t^s denotes the storage state of charge for storage s at time t. The terms e_c^s and e_d^s are efficiency constants for storage s. The state of charge and charging discharging power are bounded from above and below by their physical limits.

This storage model could furthermore be extended by adding an AC/DC converter so that the storage system can also provide reactive power for voltage support. However, for the sake of simplicity, this is not considered in the paper.

Overall, the problem is nonlinear and non-convex in each time step, and there are linear coupling constraints between the time steps.

3. Nested Benders' decomposition

In order to apply NBD, the time horizon is divided in P intervals, where the p + 1-th interval problem is considered as the slave problem of the p-th problem - or the p-th problem is considered as the master problem to the p + 1-th problem. By applying recursion this results in a chain of P optimization problems as depicted in Fig. 1.

To be more concrete, the p-th subproblem has as objective function:

$$f_p(x_p) = \sum_{t=t_{start,p}}^{t=t_{end,p}} f_t(x_t) \tag{8}$$

where t_{start}, t_{end} are the first and last time point for sub-problem p. In addition, all variable bounds hold as for the holistic problem between $t_{start,\ p}$ and $t_{end,\ p}$. The power flow constraints (4), (5) and (6) are applied as well between $t_{start,\ p}$ and $t_{end,\ p}$. As in the holistic problem, the storages energy levels at $t_{start,\ p}$ have to be given, which will be described below.

Similarly, to the sequential approach presented in [6], we use linear cuts to append to the master problems in a forward-backward-sweep

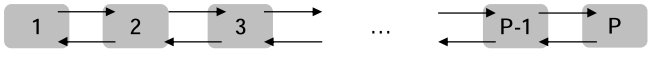

Fig. 1. Decomposition in P sub-problems with forward-backward iteration.

framework. However, it should be noted that the OPF problem in the cited paper is linear, while we consider the nonlinear and nonconvex AC power flow, so that there is no convergence proof available. In order to realize Benders' algorithm, we introduce one additional unbounded variable φ_p that is added to the objective function of each sub-problem p:

$$\tilde{f}_p(x_p) = f_p(x_p) + \varphi_p \tag{9}$$

We denote the storage energy level at time $t_{start,\ p}$ of storage s by $\underline{E}_p^s$ and the storage energy level at time $t_{end,\ p}$ of storage s in sub-problem p by $\overline{E}_p^s$. By $\overline{E}_0^s$ we denote the initial state of charge of storage s which is identical to the initial state of charge in the holistic problem.

In each iteration we add to each sub-problem except for the P-th problem a linear inequality constraint (Benders' cut) in the following form:

$$\sum_{s=1}^{S} \pi_{p+1}^s \bar{E}_p^s + \varphi_p \geq \sum_{i=1}^{M} \mu_{p+1}^i b_{p+1}^i \tag{10}$$

Here π_{p+1}^s on the left-hand side denotes the dual value for the first storage balance constraint (7) in problem $p+1$ for storage s, and the right-hand side represents the sum of all dual values of problem $p+1$ multiplied by the respective constraint or variable bounds. These dual values can be directly obtained from the solver output of the previous solution

As indicated by the arrows in Fig. 1, the algorithm consists of two main parts in each iteration:

1 Forward run: solve all sub-problems from start to end while forwarding the last storage energy level as initial energy level to the next problem
2 Backward run: solve the sub-problems from end to start while adding the cuts (10)

At the end of the forward run an upper bound for the objective value is computed:

$$\bar{z} := \sum_{p=1}^{P} f_p(x_p) \tag{11}$$

This value is equivalent to the overall objective value using the variable values from all the sub-problems.

After each backward run a lower bound is computed:

$$\underline{z}: \tilde{f}_1(x_1) = f_1(x_1) + \varphi_1 \tag{12}$$

Here φ_1 can be interpreted as the contribution of the slave problem to the objective value of master problem 1.

The overall algorithm is then as follows:

```
While z̄ − z̲ > ϵ:
For p = 1, ..., P:
E̲_p^s := Ē_{p−1}^s for s = 1, ..., S
Solve problem p
Compute z̄
For p = P − 1, ..., 1:
Add Benders' cut according to (9)
Solve problem p
Compute z̲
```

However, this approach can later be parallelized as described in the multi-stage approach in [6].

4. Numerical results

The proposed optimization scheme has been implemented in Python and uses the CaADdi framework [15] for interfacing with the IPOPT solver for nonlinear programming [16]. As an implementational sidenote, while testing, it was noted that algorithm converges to satisfactory sub-optimal solution in just a couple of iterations. Therefore, we have not explicitly used the predefined value ϵ, noted in algorithm description.

The numerical results are split in three cases [17], described below:

- Case A: test feeder IEEE13, time horizon of one day;
- Case B: test feeder IEEE37, time horizon of one week;
- Case C: test feeder IEEE123, time horizon of one week;

The aim of the numerical tests is to describe the behavior of the method in terms of robustness (i.e. comparison of the objective function with the holistic solution) and the computational burden (i.e. speed-up related to the holistic solution); moreover, for each case study, several time-division lengths of the decomposition method are shown and analyzed.

From the system point of view, the scope of the objective function is to minimize the price of energy arriving from the upper level of the grid in presence of a set of energy storages installed below the test feeder. Moreover, the IEEE test feeder data are given, in literature, as three-phase system model: for the purpose of this paper, an equivalent single-phase has been created. Details associated with these grids are shown in

4.1. IEEE 13, one day

The first case study is based on the IEEE 13 test feeder. Two storages have been connected at the nodes ID 680 and 646: the energy and power capacity are 5000/750 kWh/kW and 1000/500 respectively with a round-trip efficiency of 90% for both. The energy price, with hourly cadency, and the total feeder demand are shown in Fig. 2.

The total amount of samples is 144, equivalent to one sample every 10 minutes for 24 hours. The case is composed of 13 tests, where each one is characterized by a different number of sub-problems. In particular,Table 2 shows the problem dimensions, related to every test.

Table 3 shows the results obtained. The solution without storages is 5% more expensive: this result justifies the use of the storages in order to reach a cheaper solution.

The following table shows the results after the first and tenth iteration (the last one). One observation is that for the cases with large numbers of sub-problems, the solution after the first iteration is still close to the one without storages. In an opposite manner, decreasing the number of sub-problems, the solution at the first iteration is close to the holistic one. In each case, the objective function value, after ten iteration, is practically equal to the holistic solution.

In what regards the speed-up (ratio between computation times of holistic and NBD solution), the decomposition approach slows down the execution time of about two times after the first iteration and ten(B1)/twenty(B13) times after the tenth iteration.

Fig. 3 shows the Root Mean Square error between the holistic solution and the B7 test for each iteration and storage: the error decrease

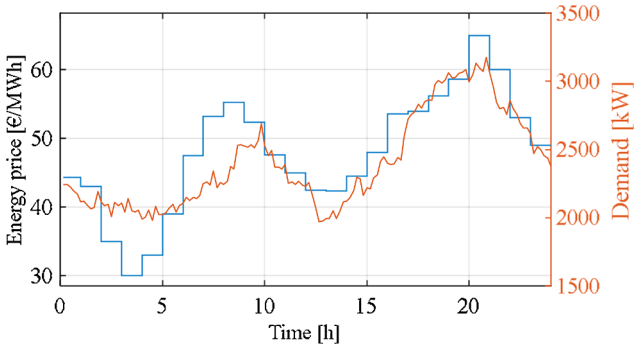

Fig. 2. Energy price and feeder demand vs time.

Table 1
Grids properties.

Properties	Values			Units
	IEEE13	IEEE37	IEEE123	
Nodes number	13	37	123	N.A.
Voltage limits [p.u.]	1.1 - 0.9			Per unit
Slack bus	650	799	150	ID
Line number	12	36	122	Per unit
Lines Ampacity	N.A.			A
Demand, day peak	3.174	3.148	2.561	MW
Demand, day energy	57.74	285.52	292.04	MWh

Table 2
Problem dimension for each test.

Test Name	Single time steps length	n. of sub problem	n. of variables	n. of constraints
Holistic solution	144	1	5184	7488
B1	2	72	73	105
B2	3	48	109	157
B3	4	36	145	209
B4	6	24	217	313
B5	8	18	289	417
B6	9	16	325	469
B7	12	12	433	625
B8	16	9	577	833
B9	18	8	649	937
B10	24	6	865	1249
B11	36	4	1297	1873
B12	48	3	1729	2497
B13	72	2	2593	3745

Table 3
Execution results.

Test Name	Obj. [%]	First iteration			Last iteration		
		Obj. (upper bound)	*Speed-up [-]*	*CPU Wall clock [s]*	*Obj. (upper bound)*	*Speed-up [-]*	*CPU Wall clock [s]*
Holistic solution	100	-	1	1.53	-	-	-
w/o storage	105	-	-	1.03	-	-	-
B1	-	104.1	0.48	3.14	100.4	0.05	27.27
B2	-	104.1	0.52	2.91	100.0	0.05	27.68
B3	-	104.1	0.55	2.78	100.1	0.06	23.40
B4	-	104.1	0.60	2.55	100.0	0.06	22.68
B5	-	103.9	0.66	2.30	100.2	0.07	20.48
B6	-	104.0	0.67	2.27	100.0	0.07	21.09
B7	-	103.9	0.71	2.16	100.0	0.07	20.05
B8	-	103.7	0.67	2.26	100.0	0.07	20.25
B9	-	103.7	0.67	2.26	100.0	0.07	20.53
B10	-	103.2	0.64	2.39	100.0	0.07	19.46
B11	-	103.1	0.73	2.07	100.0	0.08	18.33
B12	-	102.4	0.67	2.26	100.0	0.08	17.21
B13	-	100.5	0.73	2.08	100.0	0.11	13.75

monolithically for both cases.

Fig. 4 shows the energy levels between the holistic solution and the test B7, after the tenth iteration. For the storage 1, the results are identical for the first eight hours; after that, a small offset is kept between the two solutions until the end of the day. In case of storage 2, identical solution is reached after 10:00.

4.2. IEEE 37, one week

The second case study is based on the IEEE 37 test feeder. Table 4 reports the parameters of the storages installed at the distribution feeders. The storage sizes have been chosen to cover different energy/power ratio, while the round-trip efficiency used is typical for Lithium-battery (and auxiliary power electronics) technology.

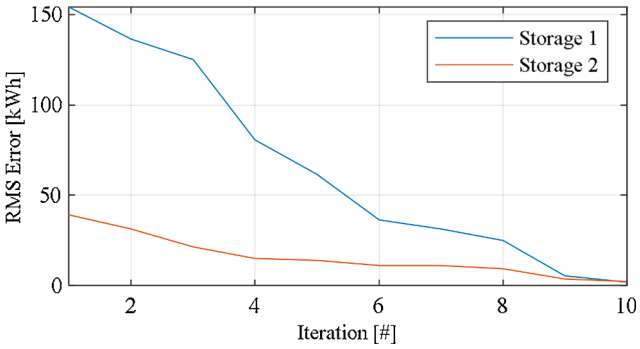

Fig. 3. RMS error of energy level vs iterations.

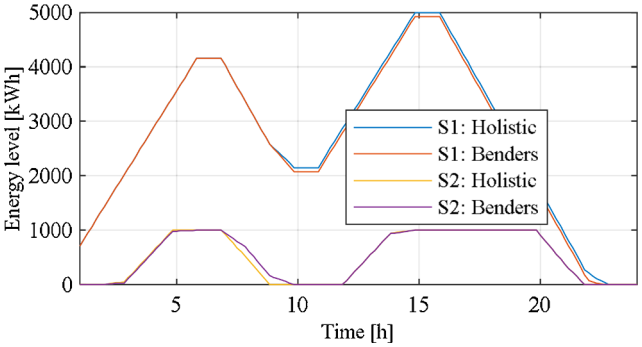

Fig. 4. Energy levels vs time.

Table 4
Storage properties.

ID	Node	E_{max} [kWh]	P_{max} [kW]	E_{start} [kWh]	η_{charge} [%]	$\eta_{cdischarge}$ [%]
1	709	5000	750	0	95	95
2	720	1000	500	0	90	98
3	737	500	750	0	98	91
4	744	50	50	0	98	95

Table 5
Problem dimension for each test.

Test Name	Single time steps length	n. of sub problem	n. of variables	n. of constraints
Holistic solution	1008	1	92736	151200
B1	3	336	227	451
B2	6	168	553	901
B3	12	84	1105	1801
B4	168	6	15457	25201
B5	252	4	23185	37801
B6	504	2	46369	75601

There is only one boundary constraint related to the initial condition of the state of charge: for this test case, it is set to zero for all the storages. Due to the direction of the objective function, the final state of charge will be automatically zero. Fig. 5 shows the total feeder demand and the hourly energy price: the last one has been artificially modified on Wednesday and Thursday in order to have different daily result; moreover, for this case the demand peak is reached during the weekend.

As in the previous case, the individual time step length is 10 min, equal to 1008 steps for one week. The case is composed of 6 tests, each one characterized by a different number of sub-problems.

Similarly to the previous case, the solution without storage is about

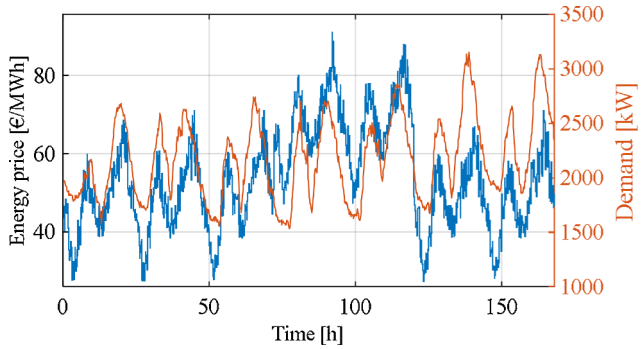

Fig. 5. Energy price and feeder demand vs time.

Table 6
Execution results.

Test Name	Obj. [%]	First iteration			Last iteration		
		Obj. (upper bound)	*Speed-up [-]*	*CPU Wall-clock [s]*	*Obj. (upper bound)*	*Speed-up [-]*	*CPU Wall-clock [s]*
Holistic solution	100	-	1	45.32	-	-	-
w/o storage	106	-	-	8.95	-	-	-
B1	-	105.3	0.80	56.08	103.5	0.08	519.19
B2	-	105.2	0.84	53.41	103.0	0.09	485.19
B3	-	105.0	0.73	61.73	102.4	0.07	571.35
B4	-	100.9	0.58	77.21	100.1	0.07	636.21
B5	-	100.7	0.77	58.16	100.0	0.09	481.56
B6	-	100.1	0.75	60.22	100.0	0.11	418.90

6% more expensive, as shown in Table 6. Comparing the holistic problem size (between case A and B), the last case is about 20 times bigger than the first.

Results of the first iteration is possible to highlight that the decomposition approach slows down the execution time (but not as much as in smaller grid case A); despite this, in the test performed we could not observe a clear monotone trend related to the problem size. The same is valid after the last iteration.

In the test cases B4, B5 and B6, the objective value is equal to the holistic solution at the end of the last iteration; for while in the other tests (B1, B2 and B3), the convergence criteria is not yet satisfied: this means that more iterations are needed when the grid size is increased and the size of the sub-problem is kept as small as possible.

Fig. 6 shows the energy state of the storage number one, after the last iteration: the holistic solution (in blue), Benders approach with sub-problem size of 504 hours (in red) and 3 hours (in orange). In the last test, the solution is not comparable with the holistic one, while the first test (2 sub-problems) with 504 hours is similar to the holistic one except for a small deviation in the middle (exactly at the interface between the

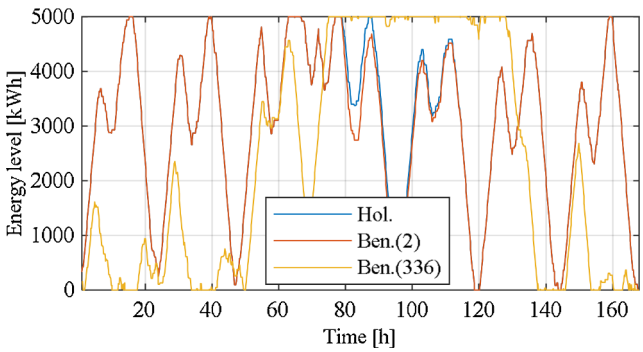

Fig. 6. Energy state of the storage 1.

Table 7
Problem dimension for each test.

Test Name	Single time steps length	n. of sub problem	n. of variables	n. of constraints
Holistic solution	1008	1	290304	508032
B1	28	36	8065	14113
B2	42	24	12097	21169
B3	56	18	16129	28225
B4	63	16	18145	31753
B5	84	12	24193	42337
B6	112	9	32257	56449
B7	126	8	36289	63505
B8	168	6	48385	84673
B9	252	4	72577	127009
B10	336	3	96769	169345
B11	504	2	145153	254017

sub-problems, where NBD passes information back and forth).

4.3. IEEE 123, one week

The third case study is based on the IEEE 123 test feeder. Table 7 reports the parameters of the storages installed in the distribution feeders.As in the previous case, ten storages have been installed at the feeder with a total amount of energy of 14.6 MWh. The same parameters pertaining to the Lithium-battery technology have been used to setup the round-trip efficiency. Table 7 shows the single test dimensions (e.g. number of constraints and variables for each sub-problem).

Table 8 reports the results obtained: the speed-up after the first iteration is around one, i.e. the first iteration takes roughly as long as the holistic solution (for the first half of tests) but the objective function is close to the solution without storages. In the last test, the solution, even in the first iteration, is close to the holistic one.

In the last iterations, the behavior of the method in terms of speed-up and objective function values is similar to the solution obtained with the small grid (Case A).

Fig. 7 shows the values of the backward and forward (lower and upper bound) objective function for the B7 test: two monotone trends are clearly shown, while the upper bound reach practically the holistic solution after the ninth iteration.

5. Conclusions and future work

In this work we applied Nested Benders' decomposition to multi-period AC-OPF in order to control distribution grids with storage systems. This problem is nonlinear and non-convex which means that there is no convergence guarantee for the method. The case studies described above indicate that the method works and gives satisfying solutions after only few iterations. The implementation of the approach demonstrates the possibility to more accurately control the distribution gird in presence of BESS.

However, there is space for improvement. The computational efficiency of the sequential execution of Nested Benders' algorithm compared to the holistic optimization problem is still sub-optimal in terms of computation time. In terms of memory demand the decomposition is favorable due to smaller problem sizes. We assume that a bigger computational speedup can be achieved by a parallel execution of the sub-problems as is proposed in [6], so this would be a natural extension of this work.

Moreover, the network control equipment can be completed, e.g. by adding battery control system that also allows reactive power support from storage devices as well as voltage regulators, etc. Additionally, the approach can be extended to include integer variables and unbalanced 3-phase grids. In the problem setting presented here the only time-coupling constraints are the storage balance constraints. The approach may as well be extended towards generator ramping constraints or

Table 8
Execution results.

Test Name	Obj. [%]	First iteration			Last iteration		
		Obj. (upper bound)	*Speed-up [-]*	*CPU Wall-clock [s]*	*Obj. (upper bound)*	*Speed-up [-]*	*CPU Wall-clock [s]*
Holistic solution	100	-	1	565.33	-	-	-
w/o storage	112	-	-	80.01	-	-	-
B1	-	110.5	1.24	454.12	102.8	0.13	4333.58
B2	-	108.7	0.97	577.04	101.8	0.09	5767.77
B3	-	107.2	1.06	531.87	101.4	0.11	5153.37
B4	-	106.7	1.00	562.88	100.6	0.12	5327.85
B5	-	105.7	0.87	642.88	100.3	0.10	6140.40
B6	-	104.4	0.82	686.41	100.3	0.09	6371.59
B7		104.0	0.77	728.91	100.1	0.09	6383.52
B8		103.1	0.82	681.08	100.1	0.10	6155.34
B9		102.2	0.70	799.20	100.0	0.10	6084.57
B10		101.6	0.64	875.30	100.0	0.10	5955.09
B11		100.5	0.65	866.31	100.0	0.12	5335.24

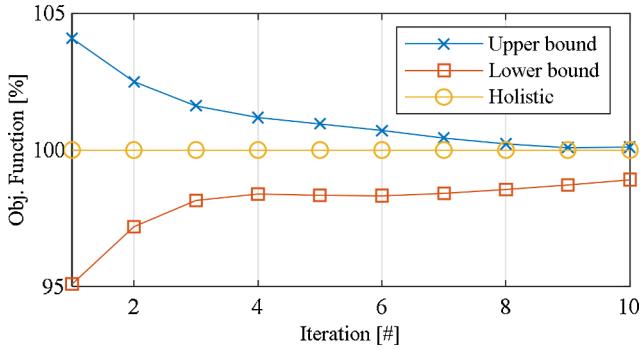

Fig. 7. Backward and forward objective function for the B7 test.

other linear relations between time steps.

Declaration of Competing Interest

The authors declare that they have no known competing financial interests or personal relationships that could have appeared to influence the work reported in this paper.

Acknowledgment

This research was partly supported by the German Federal Ministry of Education and Research (BMBF) within the framework of the project “Neue EnergieNetzStruktURen für die Energiewende” ENSURE (FKZ 03SFK1N0).

References

[1] H. Engel, R. Hensley, S. Knupfer, S. Sahdev, Charging Ahead: Electric-Vehicle Infrastructure Demand, McKinsey & Company, 2018 [Online]. Available https://www.mckinsey.com/industries/automotive-and-assembly/our-insights/charging-ahead-electric-vehicle-infrastructure-demand.
[2] J. Varela, L.J. Puglisi, T. Wiedermann, U. Ysberg, D. Stein, Z. Pokorna, C. Arnoult, R. Garaud-Verdier, L. Consiglio, Show me!: largescale smart grid demonstrations for European distribution networks, IEEE Power Energy Mag. 13 (1) (2015) 84–91.
[3] H.W. Dommel, W.F. Tinney, Optimal power flow solutions, IEEE Trans. Power Appl. Syst. -87 (10) (1968) 1866–1876 Vols. PAS.
[4] J.F. Benders, Partitioning procedures for solving mixed-variables programming problems, Numerische Mathematik 4 (I) (1962) 238–252.
[5] A.M. Geoffrion, Generalized Benders decomposition, J. Optim. Theory Appl. 10 (4) (1972) 237–260.
[6] M.V.F. Pereira, L.M.V.G. Pinto, Application of decomposition techniques to the mid- and short-term scheduling of hydrothermal systems, IEEE Trans. Power Appar. Syst. -102 (11) (1983) Vols. PAS.
[7] T.N. Santos, A.L. Diniz, A new nested benders decomposition strategy for parallel processing applied to the hydrothermal scheduling problem, IEEE Trans. Smart Grid 8 (3) (2017).
[8] S. Binato, M.V.F. Pereira, S. Granville, A new Benders decomposition approach to solve power transmission network design problems, IEEE Trans. Power Syst. 16 (2) (2001) 235–240.
[9] P. Tsamasphyrou, A. Renaud, P. Capentier, Transmission network planning under uncertainty with Benders decomposition, Lecture Notes in Economics and Mathematical Systems, Springer, Namur, 1998, pp. 457–472.
[10] H. Ma, S.M. Shahidehpour, Transmission-constrained unit commitment based on Benders decomposition, Int. J. Electr. Power Energy Syst. 20 (4) (1998) 287–294.
[11] N. Alguacil, A.J. Conejo, Multiperiod optimal power flow using benders decomposition, IEEE Trans. Power Systems 15 (1) (2000) 196–201.
[12] D. Phan, J. Kalagnanam, Some efficient optimization methods for solving the security-constrained optimal power flow problem, IEEE Trans. Power Systems 29 (2) (2014) 863–872.
[13] C.L. Lara, “Deterministic electric power infrastructure planning: mixed-integer programming model and nested decomposition algorithm, Eur. J. Oper. Res. 271 (3) (2018) 1037–1054.
[14] A. O'Connell, A. Keane, Multi-period three-phase unbalanced optimal power flow, IEEE PES ISGT (2014).
[15] J.A.E. Andersson, J. Gillis, G. Horn, J.B. Rawlings, M. Diehl, CasADi - a software framework for nonlinear optimization and optimal control, Math. Program. Comput. (2018) Chapter 5.
[16] A. Wächter, L.T. Biegler, On the implementation of a primal-dual interior point filter line search algorithm for large-scale nonlinear programming, Math. Program. 106 (1) (2006) 25–57.
[17] W.H. Kersting, Radial distribution test feeders, IEEE Trans. Power Systems 6 (3) (1991) 975–985.